

Timing of the Accreting Millisecond Pulsar XTE J1814-338

A. Papitto^{1,2*}, T.Di Salvo³, L.Burderi⁴, M.T.Menna², G.Lavagetto³ and A.Riggio^{3,4}

¹*Dipartimento di Fisica, Università degli Studi di Roma "Tor Vergata", via della Ricerca Scientifica 1, 00133 Roma, Italy*

²*Osservatorio Astronomico di Roma, via Frascati 33, Monteporzio Catone, 00040, Italy*

³*Dipartimento di Scienze Fisiche ed Astronomiche, Università di Palermo, via Archirafi 36, Palermo, 90123, Italy*

⁴*Dipartimento di Fisica, Università degli Studi di Cagliari, SP Monserrato-Sestu, KM 0.7, Monserrato, 09042 Italy*

20 August 2018

ABSTRACT

We present a precise timing analysis of the accreting millisecond pulsar XTE J1814–338 during its 2003 outburst, observed by *RXTE*. A full orbital solution is given for the first time; Doppler effects induced by the motion of the source in the binary system were corrected, leading to a refined estimate of the orbital period, $P_{orb} = 15388.7229(2)$ s, and of the projected semimajor axis, $a \sin i/c = 390.633(9)$ lt-ms. We could then investigate the spin behaviour of the accreting compact object during the outburst. We report here a refined value of the spin frequency ($\nu = 314.35610879(1)$ Hz) and the first estimate of the spin frequency derivative of this source while accreting ($\dot{\nu} = (-6.7 \pm 0.7) \times 10^{-14}$ Hz/s). This spin down behaviour arises when both the fundamental frequency and the second harmonic are taken into consideration. We discuss this in the context of the interaction between the disc and the quickly rotating magnetosphere, at accretion rates sufficiently low to allow a threading of the accretion disc in regions where the Keplerian velocity is slower than the magnetosphere velocity. We also present indications of a jitter of the pulse phases around the mean trend, which we argue results from movements of the accreting hotspots in response to variations of the accretion rate.

Key words: stars: neutron – stars: magnetic fields – pulsars: general – pulsars: individual: XTE J1814–338 – X-ray: binaries

1 INTRODUCTION

Millisecond Radio Pulsars have been long believed to be the end products of long and substantial mass transfer phases on to the neutron star in a low mass X-ray binary (hereafter LMXB; see e.g. Bhattacharya & van den Heuvel 1991). These two classes of objects are linked by the recycling scenario, that argues how an old and weakly magnetised neutron star can be effectively spun up to spin periods of few milliseconds by accretion of matter and angular momentum through a (Keplerian) accretion disc. Despite the low magnetic fields involved, these neutron stars are sufficiently fast at the end of the accretion phase to switch on again the mechanism that drives the radio pulsar phenomenon.

The absence of persistent and coherent oscillations in LMXB light curves represented for a long time an embarrassing problem for the recycling scenario, until the large collecting capabilities combined with the unprecedented temporal resolution of the Rossi X-ray Timing Explorer (*RXTE*) satellite allowed Wijnands & van der Klis (1998) to dis-

cover the first millisecond pulsar in a transient LMXB, SAX J1808.4–3658 ($P_{spin} \simeq 2.5$ ms, $P_{orb} \simeq 2$ h).

The seven accreting millisecond pulsars that have been discovered so far (Wijnands 2004; Morgan et al. 2005) have periods ranging from ~ 1.5 ms to ~ 5.5 ms, and are all harboured in very compact binary systems (orbital periods in the ~ 40 min to 4 h range) with very low mass companions ($\lesssim 0.15 M_{\odot}$). Moreover these objects have always been found in transient systems with more than 2 yr recurrence times and generally appear subluminal with respect to the other LMXBs even during their outbursts, suggesting low rates of secular mass accretion (Galloway 2006). This feature may explain why LMXBs generally do not show persistent pulsations if one lets the accretion rate to control finely the large scale magnetic field, as this would be buried under the neutron star surface when the previously unmagnetised matter accretes too rapidly for the field to diffuse through it (Cumming, Zweibel & Bildsten 2001). On the other hand at lower accretion rates, a magnetosphere can form in the neutron star surroundings, which channels the transferred matter to the magnetic poles. The radiation emitted at these spots shows the coherent and nearly sinusoidal pulsations

* E-mail: papitto@oa-roma.inaf.it

seen in X-ray light curves of accreting millisecond pulsars (hereafter AMSP).

The X-ray transient XTE J1814–338 was discovered in 2003 during scans of the central Galactic plane with RXTE (Markwardt & Swank 2003, hereafter MS03). This accreting pulsar has a 3.14 ms spin period and resides in a binary system, whose orbital period (4.275 hr) and minimum companion mass ($\simeq 0.15 M_{\odot}$) make it the widest and most massive among all the seven systems discovered so far, that harbour an AMSP.

In this paper we apply timing techniques to the persistent pulsating activity of XTE J1814–338, in order to investigate the spin frequency evolution as a result of the balance of the positive torque due to the accretion of matter and the negative torque due to the interaction between the magnetosphere and the disc.

2 OBSERVATIONS AND DATA ANALYSIS

XTE J1814–338 was found in outburst on 2003 June 5 (MJD 52795); the outburst lasted for 53 days, and had a peak (2.5–25 keV) flux of 5×10^{10} erg/cm²/s. After a smooth rise lasting for ~ 5 days, the X-ray flux showed three bumps with variations of ~ 20 per cent on a time-scale of ~ 10 days, until it suffered an abrupt cut off to one fourth of the previous average emission, 33 days from the first detection. Afterwards the source fell below the sensitivity threshold on 2003 July 27 (see upper panel of Fig.1 for the *RXTE/PCA* 2.5–25 keV light curve).

During the coverage of this outburst performed by *RXTE*, 28 thermonuclear bursts were observed, exhibiting coherent pulsations at the same period and strongly phase locked to the persistent pulsations (Strohmayer et al. 2003). Frequency variability during the course of the burst has been object of deep study, showing no relevant signs of departure from the non burst behaviour, similarly to the few Hz frequency drifts seen in other bursters as SAX J1808.4-3658 (Watts, Strohmayer & Markwardt 2005). We decided to discard an interval of 200 s following the onset of each burst. We have checked anyway that the inclusion of the bursts does not modify significantly the results of the timing.

For the timing analysis we consider data from the RXTE Proportional Counter Array (PCA, Jahoda et al. 1996), which is made of five identical units (PCUs) that yield to a total effective area of ~ 6250 cm², sensitive in the 2–60 keV energy band. We used Event mode data with 64 energy channels and a 125 μ s time resolution. First of all we corrected the photon arrival times for the motion of the spacecraft with respect to the solar system barycentre, by using JPL DE-405 ephemerides along with spacecraft ephemerides. This task was performed with the *faxbary* tool, considering as the best estimate for the source coordinates the optical counterpart position, that has a 90 per cent confidence radius of $0''.2$ (Krauss et al. 2005).

Folding light curves around the spin period 3.18110566967 ms, we detected coherent oscillations up to MJD 52844, 47 days after the first publicly available observation; an harmonic fixed at half of the spin period is clearly needed to guarantee a good fit of the pulse profiles. The ratios between the fractional amplitudes, A , of these two harmonic components and the respective uncertainties

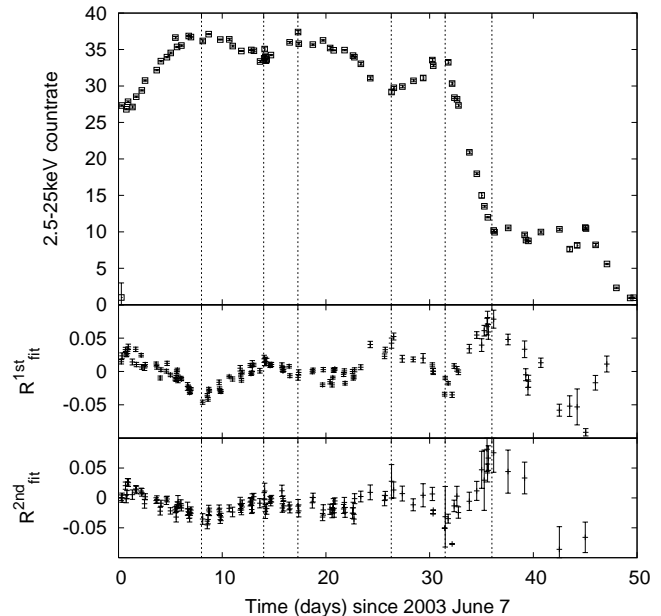


Figure 1. (2.5–25keV) light curve of the 2003 outburst of J1814, as taken by the PCA’s Unit 2 aboard RXTE, which was the only one to be on during the entire outburst. Each point represents the average count rate in every available observation, which were preliminarily background subtracted according to the faint source model (top panel). In the lower panels we plot the residuals with respect to the best-fitting constant spin down model of phase delays of the fundamental (R_{fit}^{1st} , middle panel) and of the second harmonic (R_{fit}^{2nd} , bottom panel). These plots are the same as lower panels of Fig.3 and Fig.4 respectively, and are plotted here, together with dotted vertical lines, to highlight the correlation between the shape of the light curve and the shape of the residuals of the fundamental and the second harmonic phase delays, respectively.

σ_A , are plotted in Fig.2 in order to show a measure of the significance of each detection. We note that while the fundamental frequency component is clearly above the 2σ limit until MJD 52844, the second harmonic fractional amplitude falls below this threshold ~ 35 days after the beginning of the considered observations, limiting the available number of points to perform the timing analysis upon this component.

The timing technique is able to reproduce an accurate picture of the spin behaviour of a neutron star, and is achieved by estimating the difference between the experimental time of arrival of a given pulse and the one predicted by using a certain guess of the parameters of the system, the so-called residual. The evolution in time of these residuals, depends both on the genuine variations in spin frequency and on the distance of the guessed parameters from the real ones (see e.g. Burderi et al. 2006a). Neglecting proper motion and any relativistic effect, the times of arrival of the photons are affected by various terms that can be summarised as follows: (a) the motion of the source with respect to a reference system fixed on the barycentre of the binary, (b) our inaccuracy in determining the initial spin frequency, (c) its *genuine* evolution in time and (d) the apparent motion of the source induced by the Earth orbital motion, which arises because of the uncertainty in the source position. In

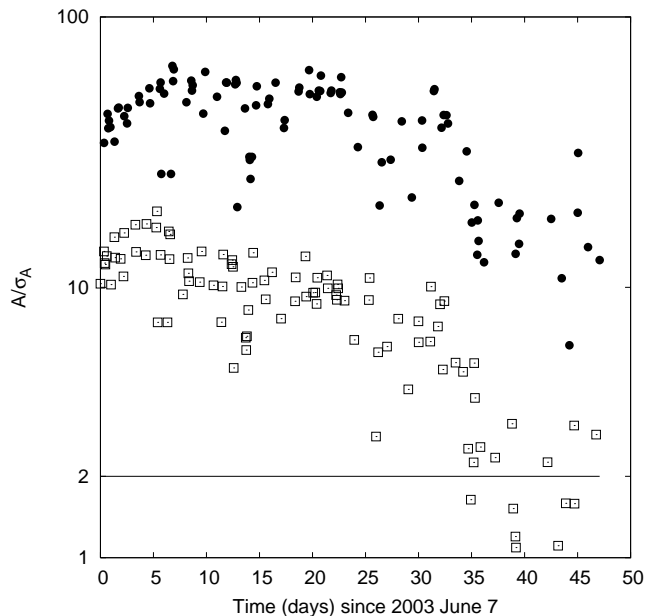


Figure 2. Ratios between the fractional amplitudes of the two considered harmonic components (filled circles refer to the fundamental frequency and squares to the second harmonic) and the relative uncertainty σ_A , plotted against the time since the first observation considered. The solid line represents the 2σ confidence level.

standard timing techniques all these effects are taken into account simultaneously, fitting the residuals with a linear multiple regression of the differential corrections of the relevant parameters (see e.g. Blandford & Teukolsky 1976).

Defining the phase as $\phi = \nu(t - T_0)$, where ν is the spin frequency and T_0 is the start time of the observation, the residuals are straightforwardly introduced as the differences between the predicted and observed phases, $R_\phi(t) = \phi_{pred}(t) - \phi_{obs}(t)$, while their evolution in time can be expressed with the relation:

$$R_\phi(t) = -\phi_0 - \delta\nu t - \delta\phi_{\dot{\nu}}(t) + R_\phi^{(orb)} + R_\phi^{(pos)}. \quad (1)$$

Here ϕ_0 is a constant, $\delta\nu$ is the correction to the frequency at the beginning of observations, and $\delta\phi_{\dot{\nu}}(t)$ is the phase variation induced by a spin frequency derivative $\dot{\nu}$, that can be expressed as a double direct integration:

$$\delta\phi_{\dot{\nu}}(t) = \int_{T_0}^t \left[\int_{T_0}^{t'} \dot{\nu}(t'') dt'' \right] dt', \quad (2)$$

so that a constant positive (negative) value of $\dot{\nu}$ leads to a quadratically decreasing (increasing) term in the phase delays evolution. The terms induced by uncertainties on orbital parameters, here labelled as $R_\phi^{(orb)}$, and on the source position, $R_\phi^{(pos)}$, are briefly discussed in the following.

Burderi et al. (2006a) showed that in the case of millisecond pulsars the timing approach is greatly simplified by the fact that the time-scale over which the terms listed above have their effect on residuals are very different. The orbital period of these systems (\sim few hours) is indeed much shorter than the timescale on which the spin period derivative seriously affects the phase delays, so that these two effects can be effectively decoupled. One can thus obtain corrections to

the initial guessed orbital parameters (namely the projected semimajor axis in light seconds $x = a \sin i/c$, the orbital period P_{orb} , the time of passage of the NS at the ascending node at the beginning of the observation T^* , and the eccentricity e) simply by fitting with the following relation the modulation that affects the pulse phases with a periodicity equal to the orbital period (see e.g. Deeter, Pravdo & Boynton 1981):

$$R_\phi^{(orb)} = \nu x \left[\sin m \frac{\delta x}{x} - \cos m \left(m \frac{\delta P_{orb}}{P_{orb}} + \frac{2\pi}{P_{orb}} \delta T^* \right) + \frac{\sin(2m)}{2} \delta e \right], \quad (3)$$

where ν is the spin frequency of the NS, $m = 2\pi(t_{arr} - T^*)/P_{orb}$ is the mean anomaly, and δx , δP_{orb} , δT^* and δe are the corrections to the respective parameters. The best orbital solution is found once the residuals are no longer modulated in this way, rather being normally distributed around the timing solution with an amplitude $\sigma_{\phi orb}$, that has to be summed in square to the statistical uncertainty affecting the phase residuals, σ_{stat} , to give the overall error on the phase determination. The expression for $\sigma_{\phi orb}$ can be evaluated simply by differentiating the formula above, substituting the differentials of the orbital parameters with their errors, and summing in quadrature:

$$\sigma_{\phi orb} = \nu x \left\{ \sin^2 m \left(\frac{\sigma_x}{x} \right)^2 + \cos^2 m \left[m^2 \left(\frac{\sigma_{P_{orb}}}{P_{orb}} \right)^2 + \left(\frac{2\pi\sigma_{T^*}}{P_{orb}} \right)^2 \right] + \sin^2(m) \cos^2(m) \sigma_e^2 \right\}^{1/2} \quad (4)$$

We therefore divided each observation in 150 s time intervals (in order to avoid a broadening of the folded pulse profiles by the orbital motion), and then fitted the phase differences according to the expression (1), without considering the position term R_ϕ^{pos} (see below), finally obtaining the orbital solution listed in Table 1. The remaining average uncertainty, that is $\langle \sigma_{\phi orb} \rangle = 0.016$ ms in our case, fairly matches the condition $\sigma_{\phi orb} \ll \delta\phi_{\dot{\nu}}(t)$, and we can therefore consider it as a "timing noise". The solution we obtain is more precise than the one already present in literature (MS03; see Tab.1) since in our analysis the entire 47 days interval was taken into consideration, and the accuracy in estimating the orbital parameters increases with the length of the time interval spanned by the data.

On the other hand, as the ephemerides of the spacecraft are supposed to be known at the highest possible accuracy, the correction for the effect induced by the Earth motion on phase residuals depends only on the uncertainty that affects the source position. This uncertainty induces delays that evolve sinusoidally on $\sim P_\oplus$ (see e.g. Lyne & Graham-Smith 1990), so that differential corrections on the source coordinates are impossible to obtain performing a timing analysis on a such short time baseline (47 days). Burderi et al. (2006a) also showed how this expression can be used to derive an upper limit on the effects of uncertainties in source coordinates over the predicted times of arrival of X-ray photons, by expanding these delays in series of the parameter $\epsilon = 2\pi(t - T_0)/P_\oplus \ll 1$. The technique there outlined leads to systematic errors affecting the linear and the quadratic terms of the time evo-

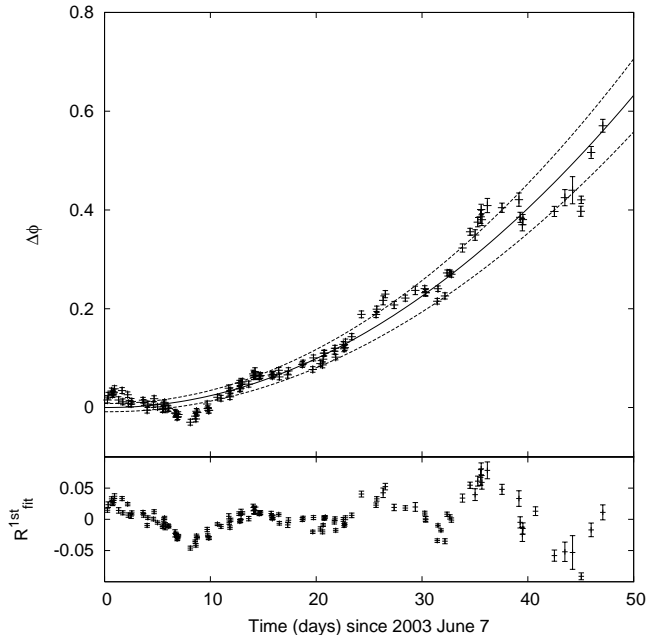


Figure 3. Evolution of the pulse phase delays, measured in their natural units, computed upon the fundamental frequency component, folding every available observation around $P = 3.18110566967$ ms. The solid line is the best fit constant $\dot{\nu}$ model, while the dashed lines represent the contours of the 90 per cent confidence region (upper panel). Residuals with respect to the best-fitting model (lower panel).

lution of the residuals, namely the spin frequency correction and the spin frequency derivative. In particular they found $\sigma_{syst \Delta\nu} \leq \nu_0 y \sigma_\gamma (1 + \sin^2 \beta)^{1/2} (2\pi/P_\oplus)$ and $\sigma_{syst \dot{\nu}} \leq \nu_0 y \sigma_\gamma (1 + \sin^2 \beta)^{1/2} (2\pi/P_\oplus)^2$, where y is the semimajor axis of the Earth's orbit in lt-s, σ_γ is the radius of the error circle on the position of the source and β is the ecliptic latitude.

Having corrected all the arrival times with our best orbital solution, we could then fold each observation around our best estimate of the barycentric spin frequency, sampling every pulse profile in 20 phase bins and finally fitting them with a two harmonics sinusoidal form. The time evolution of the phase delays, measured in their natural units (time in units of the folded spin period) of these two components are showed in Fig.3 and Fig.4, exhibiting a clear and coherent spin down trend, superimposed on which a sort of modulation is visible. A fit of the fundamental frequency phase delays evolution with a constant frequency derivative model yields to an estimate of $\langle \dot{\nu}_{fund} \rangle = (-6.7 \pm 0.7) \times 10^{-14}$ Hz/s, whose uncertainty is quoted at the 90 per cent confidence level (see below for details about its derivation). The quality of the fit is greatly affected by the modulation, whose amplitude can be estimated in $\sim 5 \langle \sigma \rangle_{fund} \simeq 0.1$ ms, leading to a very poor quality reduced chi squared ($= 1618/97$). A similar fit performed on the second harmonic phases delays, this time on a reduced number of points, as some detections result uncertain 35 days after the first observation considered here, gives slightly better results ($\chi^2 = 493/88$), as the uncertainties of the measured second harmonic phases are on the average larger than the ones of the fundamental, while the amplitude of

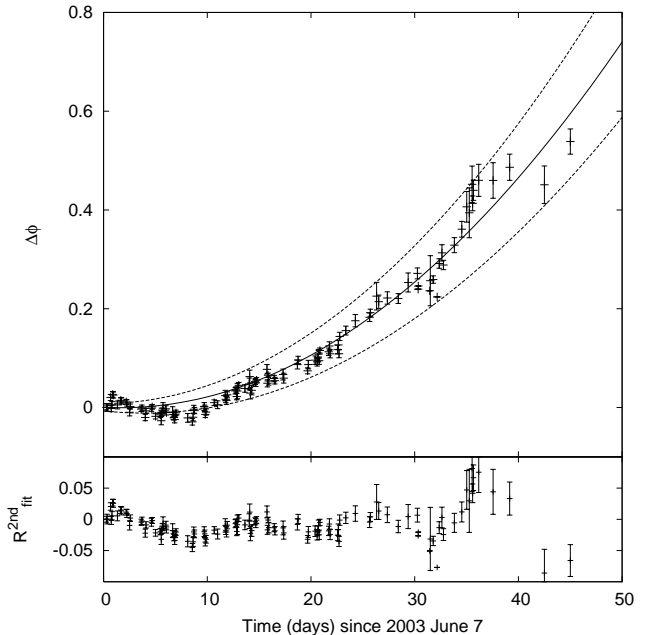


Figure 4. Evolution of the pulse phase delays, measured in their natural units, computed upon the second harmonic component, folding every available observation around $P = 3.18110566967$ ms. The solid line is the best fit constant $\dot{\nu}$ model, while the dashed lines represent the contours of the 90 per cent confidence region (upper panel). Residuals with respect to the best-fitting model (lower panel).

the modulation is just slightly smaller. The resulting estimate of the constant frequency derivative in this case is $\langle \dot{\nu}_{harm} \rangle = (-8.5 \pm 0.9) \times 10^{-14}$ Hz/s. The difference between the obtained values of $\dot{\nu}$ can be attributed to the different baseline on which the two timing analyses were performed, as the second harmonic phases are less sampled in the final part of the outburst. As a matter of fact the restriction to the first 35 days of the outburst (an interval along which the two data sets exactly overlap), yields to values of $\dot{\nu}$ that are comparable ($\dot{\nu}_{fund}^{0-35} = (-8.9 \pm 0.5) \times 10^{-14}$ Hz/s and $\dot{\nu}_{harm}^{0-35} = (-8.6 \pm 0.4) \times 10^{-14}$ Hz/s, respectively).

Beyond affecting the quality parameter of the least-square fit of the phase delays evolution, the presence of a modulation superimposed on a global spin down trend, suggests extreme caution in determining the uncertainties that affect the determination of the neutron star spin parameters, which are the frequency at the beginning of the observation and its mean derivative (σ_{ν_0} and $\sigma_{\langle \dot{\nu} \rangle}$ respectively). Rather than considering the values obtained by a simple least-square fit of the evolution of the phase delays, taken with their actual uncertainties ($\sigma_\phi = (\sigma_{\phi stat}^2 + \sigma_{\phi orb}^2)^{1/2}$), we amplified all the errors affecting the various points by a common factor (3.5 in the case of the first harmonic) until we obtain $\chi_r^2 = 1$ from the fit, and then recomputed σ_{ν_0} and $\sigma_{\langle \dot{\nu} \rangle}$ accordingly. As the relative weights of the single points remain unchanged applying this procedure, the only result is the amplification of the quoted uncertainties on the considered parameters. We believe this is appropriate in response to the presence of residuals that we do not take into account in the rotational model, but that are not

normally distributed around the timing solution nor seem to be explainable in terms of a wrong determination of the phases uncertainties (see next section). In this way we obtain values approximately 3 times larger for $\sigma_{\langle \dot{\nu} \rangle}$, which are the ones we quote throughout this paper. In Fig.3 and Fig.4 the contours of the 90 per cent confidence region are plotted with dashed lines, showing the accuracy with which the global behaviour is reproduced with these assumptions. Furthermore, considering the 90 per cent confidence radius of the position error circle ($0''.2$), the apparent motion of the source affects the determination of $\dot{\nu}$ with a systematic error $\sigma_{\text{sys} \dot{\nu}} \leq 0.6 \times 10^{-14}$ Hz/s.

3 DISCUSSION AND CONCLUSIONS

The first aspect we have to discuss is the nature of the phase jiggle that affects crucially the quality of the fit performed on the phase delays evolution plots, when either the fundamental frequency or the second harmonic is taken into consideration. This effect appears as a modulation around the mean rotational behaviour, as can be easily seen from the bottom panels of Fig.3 and Fig.4, which reproduce the residuals in their natural units from the best-fitting constant spin down model, R_{fit} , in the respective cases. The timescale of this modulation is ~ 12 days both for the fundamental and the harmonic, ruling out the possibility that this effect could be yielded by timing errors referred to a wrong position or orbital solution, as these would make the phases oscillate with very different timescales (P_{\oplus} and P_{orb} , respectively).

A striking anti-correlation can be found indeed with the shape of the X-ray light curve of the observed X-ray flux (see Fig.1). As a matter of fact when the flux increases, the residuals R_{fit} of both the fundamental and the second harmonic decrease, as the source would be spinning up, and the opposite happens when the flux decreases, as it can be seen by following dashed vertical lines in Fig.1. A linear correlation test performed on the couples of points representing the 2.5 – 25 keV count rate and R_{fit}^{1st} gives a Pearson coefficient $R = -0.80$, which for $N = 113$ points corresponds to a probability of less than 0.01 per cent for the points to be uncorrelated. We also performed a rank correlation test in order to estimate the probability of a monotonic relationship between the two observables; the Spearman coefficient we obtain is $\rho = -0.78$ with a similarly low probability of the null hypothesis. We have also checked that the maximum of the cross-correlation function between these two time series occurs in correspondence of non shift of the two series.

An attempt was made to model this behaviour as due to alternating spin up/spin down states of the NS, directly related to the varying accretion rate. However, a coherent timing solution could be found only by allowing the NS to undergo a rather crowded and unlikely series of discontinuities in the spin frequency. This is because the instantaneous value of the spin frequency with respect to the folding one, is represented by the slope of the phase time-evolution curve ($\nu(\bar{t}) = d\phi/dt|_{\bar{t}}$), so that a vertex in the $\Delta\phi$ vs t plot implies a change in the spin frequency, taking place on a time shorter than the sampling one (see for example the behaviour of the residuals R_{fit}^{1st} around the day 8 in the middle panel of Fig.1). An alternative explanation can be proposed in terms

Table 1. Orbital and spin parameters of XTE J1814-338

	MS03	This work ^a
$a \sin i/c$ (lt-ms)	390.3(3)	390.633(9)
P_{orb} (s)	15388.6(3)	15388.7229(2)
T^* (MJD)		52797.8101689(9)
Eccentricity e		$< 2.4 \times 10^{-5}$ ^b
	First Harmonic	
ν_0 (Hz)	314.35610(2)	314.35610879(1) ^c
$\langle \dot{\nu} \rangle$ (Hz/s)		$(-6.7 \pm 0.7) \times 10^{-14}$ ^d
	Second Harmonic	
ν_0 (Hz)		314.35610881(1) ^c
$\langle \dot{\nu} \rangle$ (Hz/s)		$(-8.5 \pm 0.9) \times 10^{-14}$ ^d

^a Numbers in parentheses are the uncertainties in the last significant figure at the 90 per cent confidence level.

^b 3σ upper limit

^c These frequencies refer to the beginning of the observations taken into account, MJD 52797.27387859868. The systematic error driven by position uncertainty is $\sigma_{\text{sys} \Delta\nu} \leq 3 \times 10^{-8}$ Hz and was not included in the quoted errors.

^d The systematic error driven by position uncertainty is $\sigma_{\text{sys} \dot{\nu}} \leq 6 \times 10^{-15}$ Hz/s and was not included in the quoted errors.

of the motion of accretion footprints along the NS surface, in response to variations of the accretion rate. The magnetospheric radius, R_m , is commonly defined as the radius at which the pressure exerted by the magnetic field equals the ram pressure of the accreting matter, $R_m = \phi(GM)^{-1/7} \dot{M}^{-2/7} \mu^{4/7}$, where μ is the magnetic dipole moment, and ϕ is a factor smaller than unity (see e.g. Gosh & Lamb 1991; Burderi et al. 1998). This definition gives an estimate of the radius at which accreting matter leaves the Keplerian rotational regime and starts to follow the motion of the magnetic field lines. However, it seems unlikely that this transition happens sharply, rather taking place through a finite width layer. Along this transition layer the energy densities of the magnetic field and of the matter in the disc almost equal, so that we can expect that variations in the density profile of the disc matter, witnessed by the ~ 10 days modulation in the observed X-ray flux, become able to bend at some level the magnetic flux tube along which matter reaches the hotspots on the NS surface, possibly causing an azimuthal displacement. As the hotspots rotate with the star this produces the coherent pulsations that are matter of concern of a timing analysis, so that a movement of the hotspot position results in lags of the observed phases. We therefore argue that the jitter in the phase evolution plots we observe in the 2003 outburst of XTE J1814-338 is caused by motions of the centre of the localised X-ray emission, as a result of a perturbation of the geometry of the accretion paths related to the instantaneous accretion rate. This could be particularly the case of a pulsar that spins down while accreting, if is a close interaction between the magnetic field lines and the accretion disc that makes the overall angular momentum flux to be pointed outward (see below). We note that a rather complex behaviour of the phase delays in response to variations of the instantaneous accretion rate, is also observed in the case of at least another AMSP, that is

SAX J1808.4–3658, during its 2002 outburst (Burderi et al. 2006b). A detailed description of the dynamics of the field lines in a regime of threading of the disc is beyond the scope of this paper, nevertheless a similar reasoning is proposed by Miller (1996) to explain the phase lags observed in the Bursting X-ray Pulsar GRO J1744–28 during its bursts. A similar explanation was also proposed by Galloway et al. (2001) for the variations of the dip phases in high field pulsars like GX 1+4 and RX J0812.4–3114. They estimated a $2^\circ - 6^\circ$ standard deviation of the stochastic wandering of the accretion column. On the other hand in our case the centre of the accretion spot would have been varying its longitude with an amplitude of $\sim 15^\circ$, and showing strong correlation with the observed X-ray flux. These differences in the response of the hotspot longitude to the variations of the accretion rate might be caused by the higher magnetic fields ($\sim 10^{12}G$) of those objects, which are able to control the flow of matter easier and farther from the surface. The observation of a similar effect in other accreting pulsars may provide additional insight on its nature and could eventually result in an important tool to study the interaction between the magnetic field and the falling matter, and in particular the relation between the azimuthal component of the field and the structure of the accretion disc.

Besides the appearance of this effect of phase jiggle, the general trend followed by XTE J1814–338 is a coherent spin down taking place over the whole course of the outburst. We consider the value of the spin frequency derivative computed from the timing on the fundamental frequency, $\langle \dot{\nu} \rangle = (-6.7 \pm 0.7) \times 10^{-14}$ Hz/s, as the most reliable because it was obtained on the most statistically significant data set. A spin down behaviour is also displayed by the slowest AMSP known so far ($P_S = 5.4$ ms), XTE J0929–314, whose braking rate during its 2002 outburst was estimated in $(-9.2 \pm 0.4) \times 10^{-14}$ Hz/s (Galloway et al. 2002; see also Riggio et al., in preparation, who report refined values of the orbital and spin parameters, and in particular a roughly halved value of the spin frequency derivative). This spin-down is hard to understand if one lets the torque released by accreting matter at the magnetosphere to be the only one acting on the NS, because as far as the disc rotates in the same sense of the central object the star is expected to be spun up by accretion. Models developed so far to explain the spin down behaviour showed by some accreting pulsars mostly point to the braking effect of the threading of the accretion disc by the magnetic field in regions where matter in the former rotates slower than the magnetosphere (see e.g. Gosh & Lamb 1979; Wang 1987). A similar regime can be attained in a region close to the inner edge of the disc if, thanks to a low accretion rate, the magnetosphere is allowed to expand to the corotation radius, defined as the radius at which the rotational velocity of the magnetic field lines equals the Keplerian value ($R_C = (GM/\Omega_S^2)^{1/3}$). In this case the field lines which thread the disc beyond the corotation radius spin faster than matter in its Keplerian motion. Such pulsars are referred to as "fast", because their spin frequency is so high that R_C attains values of the order of the NS radius (~ 10 km; $R_C = 36.3$ km for a $1.4M_\odot$ NS in XTE J1814–338), leaving a small room for the magnetospheric radius to remain inside the corotation limit when responding to a varying accretion rate. In the conventional propeller picture (Iarionov & Sunyaev 1975)

accretion is thought to halt whether $R_m > R_C$, because of the building of a centrifugal barrier that forbids matter to be accreted by the faster spinning magnetosphere. This scenario has been proven to be not entirely correct on an theoretical ground, as Spruit & Tamm (1993) showed how the velocity excess of the spinning magnetosphere is insufficient to drive back to infinity all the incoming matter, so that intermediate disc solutions are expected to arise when $R_m \gtrsim R_C$. In this regime matter is not entirely flung out by the centrifugal barrier, but rather builds up outside R_m and finally accretes on to the compact object, thanks to the angular momentum losses driven by the enhanced viscosity, which is assured by the higher densities involved and by the interaction between the magnetic field lines and the accretion disc. Rappaport, Fregeau & Spruit (2004) argued how the disc inner edge around a "fast" pulsar could remain fixed at the corotation radius, even if the nominal value for R_m would place the magnetospheric boundary beyond it, and showed the existence of modified Shakura & Sunyaev thin disc solutions leading to an overall outward angular momentum flux, with the disc readjusting its structure to higher densities in its inner parts. Considering a negative torque of magnetic origin, whose effect is parametrized by a factor γ , they obtain an expression for the overall torque acting on an accreting fast X-ray pulsar:

$$\tau = \dot{M}(GMR_C)^{1/2} - \gamma \frac{\mu^2}{9R_C^3} \quad (5)$$

where the first term represents the usual spin up torque guaranteed by matter accreting at R_C , and γ is a factor of the order of unity.

We use the above expression to evaluate the spin down behaviour of XTE J1814–338. The bolometric flux was estimated by Galloway, Cumming & Chakrabarty (2004), leading to a peak accretion rate of $6 \times 10^{-10} M_\odot/yr$, where the ~ 8 kpc distance estimate was considered (Strohmayer et al. 2003). During the first 35 days of the outburst the flux remained loosely constant, so that at the level of approximation at which eq.(5) was derived, we could consider its average value on this interval ($5.4 \times 10^{-10} M_\odot/yr$), and use it together with eq.(5), in order to estimate the magnetic dipole moment needed to produce such a large spin down. Expressing the overall torque as $\tau = 2\pi I \dot{\nu}$, with $I = 10^{45} g cm^2$, we obtain $\gamma^{1/2} \mu \simeq 8 \times 10^{26} G cm^3$, that corresponds to a superficial magnetic field of $B_S \simeq 8 \times 10^8 \gamma^{-1/2} G$ for a NS of 10 km of radius. This estimate is exactly in the plausible range ($10^8 - 10^9$ G) for the AMSPs to be the progenitors of radio millisecond pulsars.

REFERENCES

- Bhattacharya D., van den Heuvel E.P.J. 1991, Phys.Rep., 203, 1
 Blandford R., Teukolsky S.A. 1976, ApJ, 205, 580
 Burderi L., Di Salvo T., Robba N.R., del Sordo S., Santangelo A., Segreto A. 1998, ApJ, 498, 831
 Burderi L. et al. 2006a, ApJ, accepted (astro-ph/0611222)
 Burderi L., Di Salvo T., Menna M.T., Riggio A., Papitto A. 2006b, ApJL, in press
 Cumming A., Zweibel E., Bildsten L. 2001, ApJ, 557, 958
 Deeter J.E., Pravdo S.H., Boynton P.E. 1981, ApJ, 247, 1003
 Galloway D.K., Giles A.B., Wu K., Greenhill J.G. 2001, MNRAS, 325, 419

- Galloway D.K., Chakrabarty D., Morgan E.H., Remillard R.A. 2002, *ApJ*, 576, L137
- Galloway D.K., Cumming A., Chakrabarty D. 2004, *BAAS*, 8, 25.01
- Galloway D.K. 2006, in Braga J., D'Amico F., Rothschild R.E., eds, *Proc., The Transient Milky Way: A Perspective for ML-RAX*, AIP, Melville, NY, p.840, 50 (astro-ph/0604345)
- Gosh P., Lamb F.K. 1979, *ApJ*, 234, 296
- Gosh P., Lamb F.K. 1991, in Ventura J., Pines D., eds, *Neutron Stars: Theory and Observation*. NATO ASI Ser., Dordrecht, Kluwer, 363
- Jahoda K., et al. 1996, Siegmund O.H., Gummin M.A., eds, *Proc. SPIE Vol. 2808, EUV, X-ray, and Gamma-Ray Instrumentation for Astronomy VII*, p.59
- Krauss M.I., et al. 2005, *ApJ*, 627, 910
- Ilyarionov A.F., Sunyaev R.A. 1975, *A&A*, 39, 185
- Lyne A.G., Graham-Smith F. 1990, *Pulsar Astronomy*, Cambridge University Press
- Markwardt C.B., Swank J.H. 2003, *IAU Circ.*, 8144, 1
- Miller G.S. 1996, *ApJ*, 468, 29
- Morgan E., Kaaret P., Vanderspek R. 2005, *ATel* 523
- Rappaport S.A., Fregeau J.M., Spruit H.C. 2004, *ApJ*, 606, 436
- Spruit H.C., Tamm R.E. 1993, *ApJ*, 402, 593
- Strohmayer T.E., Markwardt C.B., Swank J.H., in 't Zand J. 2003, *ApJ*, 596, L67
- Wang Y.-M. 1987, *A&A*, 183, 257
- Watts A.L., Strohmayer T.E., Markwardt C.B. 2005, *ApJ*, 634, 547
- Wijnands R., van der Klis M. 1998, *Nature*, 394, 344
- Wijnands R. 2004, Kaaret P., Lamb F.K., Swank J.H., eds, *Proc., X-ray Timing 2003: Rossi and Beyond*, AIP, Melville, NY, p.209 (astro-ph/0403409)